A Unified Beam Finite Element Model for Extension and Shear Piezoelectric Actuation Mechanisms

Ayech Benjeddou, Marcelo A. Trindade, Roger Ohayon

A Unified Beam Finite Element Model for Extension and Shear Piezoelectric Actuation Mechanisms

A. BENJEDDOU,* M. A. TRINDADE AND R. OHAYON
Structural Mechanics and Coupled Systems Laboratory, CNAM, 2 rue Conté, 75003, Paris, France

ABSTRACT: This paper presents a finite element model for adaptive sandwich beams to deal with either *extension* or *shear actuation mechanism*. The former corresponds to an elastic core sand-wiched beam between two transversely polarized active surface layers; whereas, the latter consists of an axially polarized core, sandwiched between two elastic surface layers. For both configurations, an electric field is applied through thickness of the piezoelectric layers. The mechanical model is based on Bernoulli-Euler theory for the surface layers and Timoshenko beam theory for the core. It uses three variables, through-thickness constant deflection, and the mean and relative axial displacements of the core's upper and lower surfaces. Augmented by the bending rotation, these are the only nodal degrees of freedom of the proposed two-node adaptive sandwich beam finite element. The piezoelec-tric effect is handled through modification of the constitutive equation, when induced electric poten-tial is taken into account, and additional electric forces and moments. The proposed finite element model is validated through static and dynamic analysis of *extension* and *shear* actuated, continuous and segmented, cantilever beam configurations. Finite element results show good comparison with those found in the literature, and indicate that the newly defined *shear actuation mechanism* presents several promising features over conventional *extension actuation mechanism*, particularly for brittle piezoceramics use and energy dissipation purposes.

INTRODUCTION

SINCE the discovery of their reverse effect (actuation effect), piezoelectric materials are widely used for noise and vibration active structural control [1,8,9,16]. Crawley and de Luis [6] presented uniform-strain and Bernoulli-Euler bending analytic models for segmented piezoelectric actuators that are either bonded to an elastic substructure or embedded in a laminated composite. It was found that the force applied by the actuators consists of a passive stiffness component due to the presence of the actuator and a voltage dependent component related to the force transmitted by the piezoelectric actuator to the structure. These models were later compared to more detailed finite element models which highlighted the presence of material shear in the actuators and structures [7]. The deviation from Bernoulli-Euler model was judged to be significant for shorter, thicker actuators and for thick beams, where the influence of material shear was greatest.

Considering inertia and stiffness of surface-bounded piezoelectric materials and including effects of rotary inertia and shear deformation, Yang and Lee [17,18] developed a stepped beam model to investigate analytically, the interaction of structure vibration and piezoelectric actuation under closed-circuit conditions. Their analysis shows that a generalized stiffness from electromechanical coupling is induced in the structure system by the interaction, which leads to different natural frequency predictions compared with those at open-circuit.

The effect of coupling between longitudinal and bending deflections on the vibration of piezoelectrically sensored/actuated beams was investigated by Herman Shen [10,11] through a Timoshenko beam theory. A one-dimensional finite element formulation was also presented, consisting of two finite elements of two dof/node for the beam and five dof/node for the piezoelectric devices, assembled by a special procedure to satisfy the compatibility requirements in the vicinity of the interfaces between the piezoelectric devices and the main structure. Two additional nodal potential dofs were used for the piezoelectric finite element and the bending deflection was chosen cubic whereas longitudinal deflection and shear angle were taken linear.

Although mentioned by Soong and Hanson [14], only recently, a comparative study of a cantilevered beam, constructed using the shear mode of piezoelectric materials and the corresponding surface-mounted actuation structure, was performed by Sun and Zhang [15] using a commercial finite element analysis code. It was concluded that, for vibration control, the sandwich beam is more suitable for high-frequency and small amplitude case; whereas, the surface-mounted actuation structure may be used for the opposite case. However, from the weight consideration, the sandwich beam was found more efficient than the surface-mounted actuation structure. These results were confirmed later through a theoretical formulation [19]. It was maintained that the greatest advantage provided by the adaptive sandwich beam is its lower stresses in the actuator and along the interface be-

*Author to whom correspondence should be addressed.

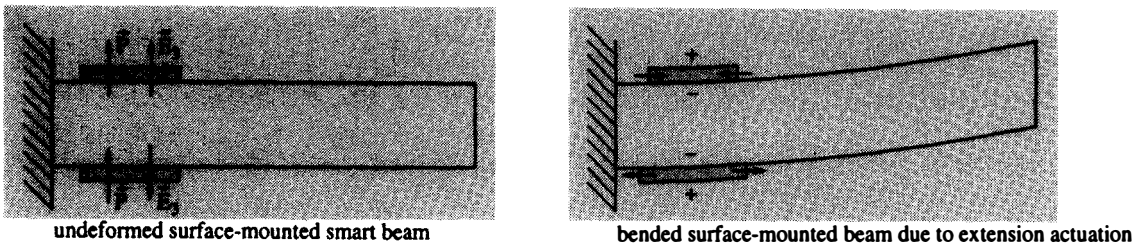

undeformed surface-mounted smart beam

bended surface-mounted beam due to extension actuation

a) extension actuation mechanism

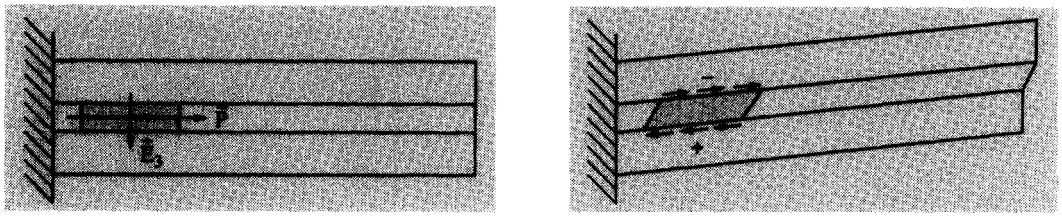

undeformed sandwich smart beam

bended sandwich beam due to shear actuation

b) shear actuation mechanism

Figure 1. *Piezoelectric actuation mechanisms.*

tween the actuator and the host structure. This fact was seen to minimize debonding problems and are known to contribute to the structural integrity of the actuator.

Surface-mounted piezoelectric actuators are known to induce longitudinal strains; this defines their usual *extension actuation mechanism* [Figure 1(a)]. However, sandwiched piezoelectric materials could induce transverse shear strains, provided that applied electric field and poling direction are perpendicular; this is the less known *shear actuation mechanism* [Figure 1(b)]. Although the so-called extension actuated adaptive structures were extensively studied in the literature, shear actuated smart structures are much less investigated.

It is the objective of the present work to present an adaptive sandwich beam finite element, capable of dealing with either *extension* or *shear actuation mechanisms*. To this end, all layers are considered piezoelectric, but the poling direction is supposed parallel to the transversely applied electric field for the faces and in the longitudinal direction for the core, i.e., perpendicular to the applied electric field. Beside, the faces are assumed unsymmetric, thin and resist membrane and bending stresses only (Bernoulli-Euler beams), whereas the core is supposed to be relatively thick and can resist membrane, bending and shear stresses (Timoshenko beam). Parametric studies [4] indicate that these hypotheses imply that the core should be softer than the faces and thick enough to produce shear stresses, and that the piezoelectric actuators are more performant for stiffer and thinner controlled structures. It was also shown in Reference [4] that there exist optimal values of faces to core stiffness and thickness ratios for maximum induced bending of the structure. The kinematics is entirely described by the transverse deflection and, the mean and relative longitudinal displacements of the upper and lower skins of the core. Augmented by the first deflection derivative, these are the only nodal degrees of freedom (dof) of the adpative sandwich element, i.e., there is no need to introduce additional electric dofs. The major contributions of the present work over that of Zhang and Sun [19] are: (1) the main variables set to describe the kinematics and the finite element degrees of freedom above; (2) the more careful and detailed formulation of the electrical problem for both actuation mechanisms, in particular the induced potential which is taken into account for the extension actuation mechanism and the description of the kind of electric loads induced by the imposed potentials for both actuation mechanisms; and (3) the uniform finite element formulation which is presented for the first time to the authors' knowledge. No finite element formulations were developed either in References [15] or [19].

THEORETICAL FORMULATION

The present sandwich adaptive beam model is based on the following assumptions:

1. Mechanical and electrical quantities are sufficiently small so that linear theories of elasticity and piezoelectricity apply.
2. Elastic and piezoelectric materials used here are considered orthotropic with axes of material symmetry coinciding with the sandwich beam axes.
3. Piezoelectric layers have their upper and lower skins fully covered with electrodes.
4. Perfect bonding occurs between layers of the sandwich structure.
5. Transverse deflection of all layers is the same at any given location in the beam thickness.

6. All layers are supposed to be in plane electrical and deformation states. Moreover, transverse stress component is considered small compared to other stress components and can be neglected.
7. The sandwich beam faces are supposed to behave as Bernoulli-Euler beams and can be either elastic or piezoelectric, poled along the thickness direction. They also may have different geometrical and material properties, i.e., the sandwich construction can be unsymmetric.
8. The sandwich beam core is considered a Timoshenko beam and can be either elastic or piezoelectric with a poling direction parallel to the longitudinal direction. Rotary inertia effects are also incorporated.

Kinematics Description

Based on the above assumptions and to the kinematics illustrated in Figure 1, this section will show that all mechanical quantities (displacements, strains, energies, . . .) can be written in terms of the transverse deflection w and the mean $\bar{u}$ and relative $\tilde{u}$ longitudinal displacements of the upper and lower skins of the core, defined as,

$$\bar{u} = \bar{u}_C = \frac{u^+ + u^-}{2}; \quad \tilde{u} = h_C \beta_C = u^+ - u^- \quad (1)$$

where $\bar{u}_C$, β_C, h_C, u^+ and u^- are, respectively, the mean displacement, bending rotation, thickness of the core and axial displacements of upper and lower skins of the core layer (Figure 2).

DISPLACEMENT FIELD EQUATIONS

Starting with linear longitudinal displacements for each layer, enforcing the interface displacement continuity conditions and using Equations (1), longitudinal displacements in the upper (A), lower (B) and core (C) layers, respectively, are

$$\begin{cases} u_A = \bar{u}_A - (z - z_A)w' \\ u_B = \bar{u}_B - (z - z_B)w' \\ u_C = \bar{u}_C + z\beta_C \end{cases} \quad (2)$$

where

$$\bar{u}_A = \bar{u} + \frac{\tilde{u}}{2} - \frac{h_A}{2} w'$$
$$\bar{u}_B = \bar{u} - \frac{\tilde{u}}{2} + \frac{h_B}{2} w' \quad (3)$$

The prime "′" denotes the first derivative with respect to the longitudinal direction x.

STRAIN-DISPLACEMENT RELATIONS

Substituting Equations (2) in the usual strain displacement relations for each layer, leads to the following axial and shear strain expressions for the upper, lower and core layers,

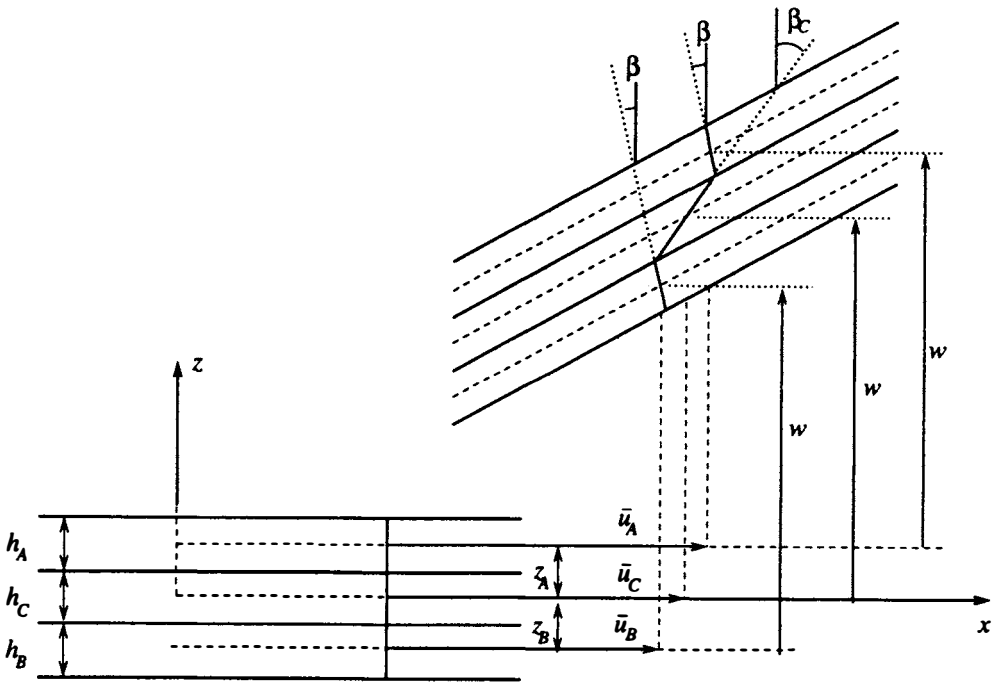

Figure 2. *Representation of the sandwich beam kinematics.*

$$\begin{aligned}
\varepsilon_{A1} &= \varepsilon_A^m + (z - z_A)\varepsilon_A^b \\
\varepsilon_{B1} &= \varepsilon_B^m + (z - z_B)\varepsilon_B^b \\
\varepsilon_{C1} &= \varepsilon_C^m + z\varepsilon_C^b \\
\varepsilon_{C5} &= \varepsilon_C^s
\end{aligned} \tag{4}$$

where the superscripts m, b and s indicate, respectively, membrane, bending and shear generalized strains. These can be written in terms of the main three variables $\bar{u}$, $\tilde{u}$ and w, as

$$\begin{aligned}
&\varepsilon_A^m = \bar{u}' + \frac{\tilde{u}'}{2} - \frac{h_A}{2} w''; \quad \varepsilon_A^b = -w''; \\
&\varepsilon_B^m = \bar{u}' - \frac{\tilde{u}'}{2} + \frac{h_B}{2} w''; \quad \varepsilon_B^b = -w''; \\
&\varepsilon_C^m = \bar{u}'; \qquad \varepsilon_C^b = \frac{\tilde{u}'}{h_C}; \quad \varepsilon_C^s = \frac{\tilde{u}}{h_C} + w'
\end{aligned} \tag{5}$$

Plane-Stress Reduced Constitutive Equations

An orthotropic piezoelectric material with material symmetry axes parallel to the beam axes is considered here. Its elastic, piezoelectric and dielectric material constants are denoted, respectively, c_{ij}, e_{kj} ($i,j = 1,\ldots,6$) and ϵ_k ($k = 1,2,3$). For both extension and shear actuated layers, a transverse electric field is applied. However, faces and core layers are treated separately, since they have different poling directions.

EXTENSION ACTUATION MECHANISM

For this case, the faces are poled in the thickness direction, i.e., parallel to the applied electric field. Mechanical and electrical assumptions for the faces, presented earlier, can be expressed mathematically as,

$$\sigma_3 = \varepsilon_2 = \varepsilon_4 = \varepsilon_5 = \varepsilon_6 = E_1 = E_2 = 0 \tag{6}$$

where σ, ε and E are stress, strain symmetric tensors and electric field vectors. Consequently, using constitutive equations [Equation (A1), cf. Appendix], the following relations also hold

$$\sigma_4 = \sigma_5 = \sigma_6 = D_1 = D_2 = 0 \tag{7}$$

Hence, constitutive equations are reduced to

$$\begin{bmatrix} \sigma_1 \\ D_3 \end{bmatrix} = \begin{bmatrix} c_{11}^* & -e_{31}^* \\ e_{31}^* & \epsilon_3^* \end{bmatrix} \begin{bmatrix} \varepsilon_1 \\ E_3 \end{bmatrix} \tag{8}$$

where D is the electric displacement vector and,

$$\begin{aligned}
c_{11}^* &= c_{11} - \frac{c_{13}^2}{c_{33}}; \quad e_{31}^* = e_{31} - \frac{c_{13}}{c_{33}} e_{33}; \\
\epsilon_3^* &= \epsilon_3 + \frac{e_{31}^2}{c_{33}}
\end{aligned} \tag{9}$$

This modification is only due to the plane stress assumption ($\sigma_3 = 0$); other nonvanishing components σ_2 and ε_3 do not contribute to the electromechanical energy. Notice that the electromechanical coupling is between axial strain and transverse electric field component only. This is the basic foundation of the extension or surface-mounted actuators.

SHEAR ACTUATION MECHANISM

Using core's mechanical and electrical assumptions, that can be written as

$$\sigma_3 = \varepsilon_2 = \varepsilon_4 = \varepsilon_6 = E_1 = E_2 = 0 \tag{10}$$

leads to the following relations, according to constitutive equations [Equation (A2), cf. Appendix],

$$\sigma_4 = \sigma_6 = D_2 = 0 \tag{11}$$

Hence, three-dimensional constitutive equations reduce to,

$$\begin{bmatrix} \sigma_1 \\ \sigma_5 \\ D_3 \end{bmatrix} = \begin{bmatrix} c_{33}^* & 0 & 0 \\ 0 & c_{55} & -e_{15} \\ 0 & e_{15} & \epsilon_1 \end{bmatrix} \begin{bmatrix} \varepsilon_1 \\ \varepsilon_5 \\ E_3 \end{bmatrix} \tag{12}$$

where

$$c_{33}^* = c_{33} - \frac{c_{13}^2}{c_{11}} \tag{13}$$

This modification is also due to the plane stress assumption for the core ($\sigma_3 = 0$). Notice that the electromechanical coupling is between shear strain and transverse electric field component only. This is the origin of the newly defined concept of *shear actuation mechanism*.

Electric State Description

This section aims to define the electric potential form in the faces and in the core for *extension* and *shear actuation mechanisms*. Electric field equations are then deduced for each case. Due to the different electric behavior of the faces and the core, *extension* and *shear actuation mechanisms* are also studied separately.

EXTENSION ACTUATION MECHANISM

For free volumic charge density assumption, the electrostatic equilibrium equation of the ith face layer reduces to

$$D_{i3,3} = 0 \tag{14}$$

since $D_{i1} = D_{i2} = 0$, according to Equation (7). Axial strains and electric field, written in terms of axial and transverse displacements and the electric potential, respectively, are

$$\varepsilon_{i1} = \bar{u}_i' - (z - z_i)w''; \quad E_{i3} = -\partial_z \varphi_i \tag{15}$$

These equations combined with direct effect from Equation (8), and included in Equation (14), lead to a quadratic electric potential form in the faces,

$$\varphi_i = \bar{\varphi}_i + (z - z_i)\frac{\tilde{\varphi}_i}{h_i} + \left(1 - \frac{4(z - z_i)^2}{h_i^2}\right)\frac{h_i^2}{8}\frac{e_{31}^{i*}}{\epsilon_3^{i*}} w'' \tag{16}$$

where

$$\bar{\varphi}_i = \frac{\varphi_i^+ + \varphi_i^-}{2}; \quad \tilde{\varphi}_i = \varphi_i^+ - \varphi_i^- \tag{17}$$

φ_i^+ and φ_i^- are prescribed electric potentials on the upper and lower skins of the ith face, respectively and h_i is the ith face thickness. Hence, $\bar{\varphi}_i$ and $\tilde{\varphi}_i$ state the mean and relative (or difference) potential of the ith face.

As was shown in a previous paper [13], the electric potential in the faces, given by Equation (16), is the sum of a linear part, entirely determined through the prescribed potentials $\varphi^{\pm}$, and a quadratic part, proportional to the beam bending strain. The latter part represents the induced potential, often neglected in the literature. It depends on geometrical and material properties.

From Equation (16) transverse electric field components on the upper and lower faces are

$$E_{i3} = -\frac{\tilde{\varphi}_i}{h_i} + (z - z_i)\frac{e_{31}^{i*}}{\varepsilon_3^{i*}} w''; \quad i = A,B \tag{18}$$

Notice that the electric field is linear in the faces. The second part of Equation (18) is often neglected in the literature. It represents the induced electric field.

SHEAR ACTUATION MECHANISM

The same above approach is used for the core layer. Considering that $D_{C1,1}$ is negligible, compared to $D_{C3,3}$, Equation (14) also holds here, since D_{C2} vanishes, according to Equation (11). Then, using direct effect of Equation (12), in conjunction with the transverse electric field definition [Equation (15)], the electric potential in the core is shown to be linear in the thickness direction, since transverse shear strain is constant [cf. Equation (5)], i.e.,

$$\varphi_C = \bar{\varphi}_C + z\frac{\tilde{\varphi}_C}{h_C} \tag{19}$$

where $\bar{\varphi}_C$ and $\tilde{\varphi}_C$ are now the mean and relative potentials of the core layer and h_C, its thickness.

It is worthwhile to notice here that the simplifying assumption on $D_{C1,1}$ leads to a negligible induced potential.

From the above equation, the transverse electric field component in the core layer is simply

$$E_{C3} = -\frac{\tilde{\varphi}_C}{h_C} \tag{20}$$

In this case the electric field is constant through the core layer.

Variational Formulation of the Problem

The variational formulation of the adaptive piezoelectric sandwich beam can be expressed as

$$\delta T - \delta H + \delta W = 0 \tag{21}$$

where δT, δH and δW are the virtual variations of kinetic energy, electromechanical energy and work done by external forces, respectively. Each of these quantities can be expressed in terms of the main variables $\bar{u}$, $\tilde{u}$, w, for an actuation problem [2]. However, for a sensoring problem, $\tilde{\varphi}_i$ should be included as main variable.

ELECTROMECHANICAL ENERGY VARIATION

Starting from the electromechanical energy of a piezoelectric media of volume V,

$$H = \frac{1}{2}\int_V (\sigma\varepsilon - DE)dV \tag{22}$$

then using constitutive Equations (8) and (12) and strain and electric field relations [Equations (4) and (15)], and integrating through thickness, the above equation becomes

$$H = H_A + H_B + H_C \tag{23}$$

where

$$H_i = \frac{1}{2}\int_0^L \left[c_{11}^{i*} A_i (\varepsilon_i^m)^2 + \bar{c}_{11}^i I_i (\varepsilon_i^b)^2 + 2e_{31}^{i*} A_i \varepsilon_i^m \frac{\tilde{\varphi}_i}{h_i} - \epsilon_3^{i*} A_i \left(\frac{\tilde{\varphi}_i}{h_i}\right)^2 \right] dx; \quad i = A,B \tag{24}$$

$$H_C = \frac{1}{2}\int_0^L \Bigg[c_{33}^{C*} A_C (\varepsilon_C^m)^2 + c_{33}^{C*} I_C (\varepsilon_C^b)^2 + c_{55}^C A_C (\varepsilon_C^s)^2 + 2e_{15}^C A_C \varepsilon_C^s \frac{\widetilde{\varphi}_C}{h_C} - \epsilon_1^C A_C \left(\frac{\widetilde{\varphi}_C}{h_C}\right)^2 \Bigg] dx \tag{25}$$

and

$$\bar{c}_{11}^i = c_{11}^{i*} + \frac{(e_{31}^{i*})^2}{\epsilon_3^{i*}} \tag{26}$$

is a newly modified elastic constant. This modification is now due to the induced electric potential effect. I_i and A_i are the moment inertia and area of the ith layer. Notice that the electromechanical coupling for the faces ($i=A,B$) is between membrane strains and imposed transverse electric field $\widetilde{\varphi}_i/h_i$ due to piezoelectric modified constants e_{31}^{i*}. However, for the core it is between transverse shear strain ε_C^s and applied transverse electric field, due to the piezoelectric coupling constant e_{15}^C.

Reorganization and variation of H leads to

$$\begin{aligned}\delta H = \int_0^L \Bigg\{ & \Big[c_{11}^{A*} A_A \delta\varepsilon_A^m \varepsilon_A^m + c_{11}^{B*} A_B \delta\varepsilon_B^m \varepsilon_B^m \\ & + c_{33}^{C*} A_C \delta\varepsilon_C^m \varepsilon_C^m + \bar{c}_{11}^A I_A \delta\varepsilon_A^b \varepsilon_A^b + \bar{c}_{11}^B I_B \delta\varepsilon_B^b \varepsilon_B^b \\ & + c_{33}^{C*} I_C \delta\varepsilon_C^b \varepsilon_C^b + c_{55}^C A_C \delta\varepsilon_C^s \varepsilon_C^s \Big] \\ & + \Bigg[e_{31}^{A*} A_A \delta\varepsilon_A^m \frac{\widetilde{\varphi}_A}{h_A} + e_{31}^{B*} A_B \delta\varepsilon_B^m \frac{\widetilde{\varphi}_B}{h_B} \\ & + e_{15}^C A_C \delta\varepsilon_C^s \frac{\widetilde{\varphi}_C}{h_C} + e_{31}^{A*} A_A \frac{\delta\widetilde{\varphi}_A}{h_A} \varepsilon_A^m \\ & + e_{31}^{B*} A_B \frac{\delta\widetilde{\varphi}_B}{h_B} \varepsilon_B^m + e_{15}^C A_C \frac{\delta\widetilde{\varphi}_C}{h_C} \varepsilon_C^s \Bigg] \\ & - \Bigg[\epsilon_3^{A*} A_A \frac{\delta\widetilde{\varphi}_A}{h_A} \frac{\widetilde{\varphi}_A}{h_A} + \epsilon_3^{B*} A_B \frac{\delta\widetilde{\varphi}_B}{h_B} \frac{\widetilde{\varphi}_B}{h_B} \\ & + \epsilon_1^C A_C \frac{\delta\widetilde{\varphi}_C}{h_C} \frac{\widetilde{\varphi}_C}{h_C} \Bigg] \Bigg\} dx \end{aligned} \tag{27}$$

The above equation holds for either actuation or sensing; for the former case, $\delta\widetilde{\varphi}_i = 0$, whereas for the latter $\delta\widetilde{\varphi}_i \neq 0$, $i = A,B,C$.

Expression (27) of the electromechanical energy variation can be split into four parts

$$\delta H = \delta H_m + \delta H_{me} + \delta H_{em} + \delta H_e \tag{28}$$

where δH_m, δH_e, δH_{me} and δH_{em} are the mechanical, dielectric and piezoelectric coupling terms of δH,

$$\begin{aligned}\delta H_m = \int_0^L \Big[& \Big(c_{11}^{A*} A_A \delta\varepsilon_A^m \varepsilon_A^m + c_{11}^{B*} A_B \delta\varepsilon_B^m \varepsilon_B^m \\ & + c_{33}^{C*} A_C \delta\varepsilon_C^m \varepsilon_C^m \Big) + \Big(\bar{c}_{11}^A I_A \delta\varepsilon_A^b \varepsilon_A^b + \bar{c}_{11}^B I_B \delta\varepsilon_B^b \varepsilon_B^b \\ & + c_{33}^{C*} I_C \delta\varepsilon_C^b \varepsilon_C^b \Big) + c_{55}^C A_C \delta\varepsilon_C^s \varepsilon_C^s \Big] dx \\ \delta H_{me} = \int_0^L \Bigg[& e_{31}^{A*} A_A \delta\varepsilon_A^m \frac{\widetilde{\varphi}_A}{h_A} + e_{31}^{B*} A_B \delta\varepsilon_B^m \frac{\widetilde{\varphi}_B}{h_B} \\ & + e_{15}^C A_C \delta\varepsilon_C^s \frac{\widetilde{\varphi}_C}{h_C} \Bigg] dx \\ \delta H_{em} = \int_0^L \Bigg[& e_{31}^{A*} A_A \frac{\delta\widetilde{\varphi}_A}{h_A} \varepsilon_A^m + e_{31}^{B*} A_B \frac{\delta\widetilde{\varphi}_B}{h_B} \varepsilon_B^m \\ & + e_{15}^C A_C \frac{\delta\widetilde{\varphi}_C}{h_C} \varepsilon_C^s \Bigg] dx \\ \delta H_e = -\int_0^L \Bigg[& \epsilon_3^{A*} A_A \frac{\delta\widetilde{\varphi}_A}{h_A} \frac{\widetilde{\varphi}_A}{h_A} + \epsilon_3^{B*} A_B \frac{\delta\widetilde{\varphi}_B}{h_B} \frac{\widetilde{\varphi}_B}{h_B} \\ & + \epsilon_1^C A_C \frac{\delta\widetilde{\varphi}_C}{h_C} \frac{\widetilde{\varphi}_C}{h_C} \Bigg] dx \end{aligned} \tag{29}$$

Strain-displacement Relations (5) are substituted in Equation (27) in order to express its variation in terms of the main variables $\bar{u}$, $\widetilde{u}$, w and $\widetilde{\varphi}$ only.

$$\begin{aligned}\delta H = \int_0^L \Bigg\{ & \Bigg[\Big(c_{11}^{A*} A_A + c_{11}^{B*} A_B + c_{33}^{C*} A_C \Big) \bar{u}' \\ & + \frac{1}{2}\Big(c_{11}^{A*} A_A - c_{11}^{B*} A_B \Big) \widetilde{u}' - \frac{1}{2}\Big(c_{11}^{A*} A_A h_A \\ & - c_{11}^{B*} A_B h_B \Big) w'' + e_{31}^{A*} A_A \frac{\widetilde{\varphi}_A}{h_A} + e_{31}^{B*} A_B \frac{\widetilde{\varphi}_B}{h_B} \Bigg] \delta\bar{u}' \\ & + \Bigg[\frac{1}{2}\Big(c_{11}^{A*} A_A - c_{11}^{B*} A_B \Big) \bar{u}' + \frac{1}{4}\Big(c_{11}^{A*} A_A \end{aligned} \tag{30}$$

$$+ c_{11}^{B*} A_B + c_{33}^{C*} \frac{4I_C}{h_C^2}\Big)\widetilde{u}' - \frac{1}{4}\Big(c_{11}^{A*} A_A h_A$$

$$+ c_{11}^{B*} A_B h_B\Big) w'' + \frac{1}{2}\Big(e_{31}^{A*} A_A \frac{\widetilde{\varphi}_A}{h_A}$$

$$- e_{31}^{B*} A_B \frac{\widetilde{\varphi}_B}{h_B}\Big)\Big]\delta\widetilde{u}' - \Big[\frac{1}{2}\Big(c_{11}^{A*} A_A h_A$$

$$- c_{11}^{B*} A_B h_B\Big)\overline{u}' + \frac{1}{4}\Big(c_{11}^{A*} A_A h_A + c_{11}^{B*} A_B h_B\Big)\widetilde{u}'$$

$$- \frac{1}{4}\Big(c_{11}^{A*} A_A h_A^2 + c_{11}^{B*} A_B h_B^2 + 4\overline{c}_{11}^{A} I_A$$

$$+ 4\overline{c}_{11}^{B} I_B\Big) w'' + \frac{1}{2}\Big(e_{31}^{A*} A_A \widetilde{\varphi}_A - e_{31}^{B*} A_B \widetilde{\varphi}_B\Big)\Big]\delta w''$$

$$+ \Big[c_{55}^{C} \frac{A_C}{h_C}\Big(\frac{\widetilde{u}}{h_C} + w'\Big) + e_{15}^{C} \frac{A_C}{h_C} \frac{\widetilde{\varphi}_C}{h_C}\Big]\delta\widetilde{u}$$

$$+ \Big[c_{55}^{C} A_C \Big(\frac{\widetilde{u}}{h_C} + w'\Big) + e_{15}^{C} A_C \frac{\widetilde{\varphi}_C}{h_C}\Big]\delta w'$$

$$+ \Big[e_{31}^{A*} \frac{A_A}{h_A}\Big(\overline{u}' + \frac{\widetilde{u}'}{2} - \frac{h_A}{2} w''\Big)$$

$$- \epsilon_3^{A*} \frac{A_A}{h_A} \frac{\widetilde{\varphi}_A}{h_A}\Big]\delta\widetilde{\varphi}_A + \Big[e_{31}^{B*} \frac{A_B}{h_B}\Big(\overline{u}' - \frac{\widetilde{u}'}{2} + \frac{h_B}{2} w''\Big)$$

$$- \epsilon_3^{B*} \frac{A_B}{h_B} \frac{\widetilde{\varphi}_B}{h_B}\Big]\delta\widetilde{\varphi}_B + \Big[e_{15}^{C} \frac{A_C}{h_C}\Big(\frac{\widetilde{u}}{h_C} + w'\Big)$$

$$- \epsilon_1^{C} \frac{A_C}{h_C} \frac{\widetilde{\varphi}_C}{h_C}\Big]\delta\widetilde{\varphi}_C\Big\} dx \qquad \text{(30 cont.)}$$

KINETIC ENERGY VARIATION

For the sandwich adaptive beam, the kinetic energy is defined as

$$T = \frac{1}{2}\int_V \rho_i\big(\dot{u}_i^2 + \dot{w}_i^2\big) dV; \quad i = A,B,C \qquad (31)$$

where ρ_i is the volumic mass density of the ith layer and the dot symbol $(\cdot)$ stands for time derivation and $w_i = w$ for $i = A,B,C$.

Substituting displacements by their Expressions (2) and integrating on the beam's thickness, lead to

$$T = \frac{1}{2}\int_0^L \rho_A\Big[A_A\big((\dot{\overline{u}}_A)^2 + \dot{w}^2\big) + I_A(\dot{w})^2\Big]$$

$$+ \rho_B\Big[A_B\big((\dot{\overline{u}}_B)^2 + \dot{w}^2\big) + I_B(\dot{w})^2\Big]$$

$$+ \rho_C\Big[A_C\big((\dot{\overline{u}}_C)^2 + \dot{w}^2\big) + I_C\dot{\beta}_C^2\Big]\Big\} dx \qquad (32)$$

We then may obtain the variation of T

$$\delta T = -\int_0^L \Big\{\rho_A\Big[A_A\big(\delta\overline{u}_A\ddot{\overline{u}}_A + \delta w\ddot{w}\big) + I_A\delta w'\ddot{w}'\Big]$$

$$+ \rho_B\Big[A_B\big(\delta\overline{u}_B\ddot{\overline{u}}_B + \delta w\ddot{w}\big) + I_B\delta w'\ddot{w}'\Big]$$

$$+ \rho_C\Big[A_C\big(\delta\overline{u}_C\ddot{\overline{u}}_C + \delta w\ddot{w}\big) + I_C\delta\beta_C\ddot{\beta}_C\Big]\Big\} dx \qquad (33)$$

Mean displacements are substituted by their Expressions (2), in Equation (33), in order to allow Equation (33) to be written in terms of the main variables $\overline{u}$, $\widetilde{u}$ and w, only

$$\delta T = -\int_0^L \Big\{\Big[(\rho_A A_A + \rho_B A_B + \rho_C A_C)\ddot{\overline{u}} + \frac{1}{2}(\rho_A A_A$$

$$- \rho_B A_B)\ddot{\widetilde{u}} - \frac{1}{2}(\rho_A A_A h_A - \rho_B A_B h_B)\ddot{w}'\Big]\delta\overline{u}$$

$$+ \Big[\frac{1}{2}(\rho_A A_A - \rho_B A_B)\ddot{\overline{u}}$$

$$+ \frac{1}{4}\Big(\rho_A A_A + \rho_B A_B + \rho_C \frac{4I_C}{h_C^2}\Big)\ddot{\widetilde{u}} - \frac{1}{2}(\rho_A A_A h_A$$

$$+ \rho_B A_B h_B)\ddot{w}'\Big]\delta\widetilde{u} + (\rho_A A_A + \rho_B A_B$$

$$+ \rho_C A_C)\ddot{w}\delta w - \Big[\frac{1}{2}(\rho_A A_A h_A - \rho_B A_B h_B)\ddot{\overline{u}}$$

$$+ \frac{1}{2}(\rho_A A_A h_A + \rho_B A_B h_B)\ddot{\widetilde{u}} - \frac{1}{4}(\rho_A A_A h_A^2$$

$$+ \rho_B A_B h_B^2 + 4\rho_A I_A + 4\rho_B I_B)\ddot{w}'\Big]\delta w'\Big\} dx \qquad (34)$$

VARIATION OF THE WORK OF EXTERNAL MECHANICAL FORCES

Each layer of the adaptive sandwich structure can be subjected to normal and transversal surface forces T_N^i and T_Q^i and to normal and transversal body forces t_N^i and t_Q^i, respectively. The work due to these forces can be written as

$$W = \left[\int_{A_i}\left(T_N^i u_i + T_Q^i w\right) dA_i\right]\Big|_0^L$$

$$+ \int_{V_i}\left(t_N^i u_i + t_Q^i w\right) dV_i; \quad i = A,B,C \tag{35}$$

Using displacement Expressions (2) and integrating this expression on the beam thickness, we obtain

$$W = \left[(N_A \bar{u}_A - M_A w' + Q_A w) + (N_B \bar{u}_B - M_B w'\right.$$

$$\left. + Q_B w) + (N_C \bar{u}_C + M_C \beta_C + Q_C w)\right]_0^L$$

$$+ \int_0^L \left[(n_A \bar{u}_A - m_A w' + q_A w) + (n_B \bar{u}_B - m_B w'\right.$$

$$\left. + q_B w) + (n_C \bar{u}_C + m_C \beta_C + q_C w)\right] dx \tag{36}$$

where classical definitions of stress resultants are used for point forces and moments,

$$N_i = \int_{A_i} T_N^i \, dA_i, \quad M_i = \int_{A_i} T_N^i (z - z_i) dA_i,$$

$$Q_i = \int_{A_i} T_Q^i dA_i \tag{37}$$

for $i = A,B,C$ and $z_C = 0$. Also distributed forces and moments are defined by

$$n_i = \int_{A_i} t_N^i \, dA_i, \quad m_i = \int_{A_i} t_N^i (z - z_i) dA_i,$$

$$q_i = \int_{A_i} t_Q^i dA_i \tag{38}$$

A variation of Equation (36) gives

$$\delta W = [N_A \delta \bar{u}_A - M_A \delta w' + Q_A \delta w + N_B \delta \bar{u}_B - M_B \delta w'$$

$$+ Q_B \delta w + N_C \delta \bar{u}_C + M_C \delta \beta_C + Q_C \delta w]_0^L$$

$$+ \int_0^L [n_A \delta \bar{u}_A - m_A \delta w' + q_A \delta w + n_B \delta \bar{u}_B$$

$$- m_B \delta w' + q_B \delta w + n_C \delta \bar{u} + m_C \delta \beta_C + q_C \delta w] dx \tag{39}$$

and use of Relation (2) gives the following expression in terms of the main variables,

$$\delta W = \left[(N_A + N_B + N_C)\delta \bar{u} + \left(\frac{N_A - N_B}{2} + \frac{M_C}{h_C}\right)\delta \tilde{u}\right.$$

$$- \left(\frac{N_A h_A - N_B h_B}{2} + M_A + M_B\right)\delta w'$$

$$\left. + (Q_A + Q_B + Q_C)\delta w\right]_0^L$$

$$+ \int_0^L \left[(n_A + n_B + n_C)\delta \bar{u} + \left(\frac{n_A - n_B}{2} + \frac{m_C}{h_C}\right)\delta \tilde{u}\right.$$

$$- \left(\frac{n_A h_A - n_B h_B}{2} + m_A + m_B\right)\delta w'$$

$$\left. + (q_A + q_B + q_C)\delta w\right] dx \tag{40}$$

VARIATIONAL FORMULATION OF THE ACTUATION PROBLEM

For the actuation problem, $\tilde{\varphi}_i$ is known (imposed), hence their variations $\delta\tilde{\varphi}_i$ vanish. It is clear then that δH_e and δH_{em}, defined in Equations (28) and (29), also vanish and Equation (28) reduces to

$$\delta H = \delta H_m + \delta H_{me} \tag{41}$$

Substitution of this relation in Equation (21) gives

$$\delta H_m - \delta T = \delta W - \delta H_{me} \tag{42}$$

where δH_{me} can be seen as a virtual work of induced electric forces and moments. It can also be interpreted as the work of "initial" electrical stresses.

In summary, the piezoelectric effect appears in the modification of the bending behavior through the modified elastic constants $\bar{c}_{11}^i$, present in δH_m, and in an additional equivalent work of electrical forces δH_{me}. Consequently, there is no need for electrical degrees of freedom for the finite element formulation, which will be based on Equation (42). It is also worthy to notice that, for an actuation problem, electrical boundary conditions affect the equivalent electric work only through the modification of the electric "initial" electric state.

The practical case of symmetric construction (identical surface layers) was briefly discussed in Reference [2] and detailed in Reference [4]. In particular, it was found that the main fundamental difference between *extension* and *shear actuation mechanisms* is that the former acts through boundary point axial forces and bending moments; whereas, the latter acts through distributed interface shear forces and bending moments [4].

FINITE ELEMENT FORMULATION

The aim of this section is to present the finite element formulation for the actuation problem. As the variations are written in terms of the main variables $\bar{u}$, $\tilde{u}$ and w, Lagrange linear shape functions were used for $\bar{u}$, $\tilde{u}$, since they are C^0-continuous, and Hermite cubic ones for w, since it is C^1-continuous.

Using Equation (29), the discretized form of the variation δH_m can be written as

$$\delta H_m = \delta q^T K q \tag{43}$$

where K is the stiffness matrix of the adaptive sandwich beam, given by,

$$K = \int_0^L \Big[c_{11}^{A*} A_A B_{Am}^T B_{Am} + c_{11}^{B*} A_B B_{Bm}^T B_{Bm} + c_{33}^{C*} A_C B_{Cm}^T B_{Cm} + (\bar{c}_{11}^{A} I_A + \bar{c}_{11}^{B} I_B) B_{ABb}^T B_{ABb} + c_{33}^{C*} I_C B_{Cb}^T B_{Cb} + c_{55}^{C} A_C B_{Cs}^T B_{Cs} \Big] dx \tag{44}$$

and q is the dof-vector defined by

$$q = \left[\bar{u}_1, \tilde{u}_1, w_1, w_1', \bar{u}_2, \tilde{u}_2, w_2, w_2' \right]^T \tag{45}$$

T states for transpose operation and B_{ij}, $i = A,B,C, j = m,b,s$ are deformation matrices for membrane, bending and shear, respectively.

Discretization of the kinetic energy variation [Equation (33)] is,

$$\delta T = \delta q^T M \ddot{q} \tag{46}$$

where M is the mass matrix of the adaptive sandwich beam element,

$$M = \int_0^L \Big[\rho_A A_A B_{Atx}^T B_{Atx} + \rho_B A_B B_{Btx}^T B_{Btx} + \rho_C A_C B_{Ctx}^T B_{Ctx} + (\rho_A A_A + \rho_B A_B + \rho_C A_C) B_{tz}^T B_{tz} + (\rho_A I_A + \rho_B I_B) B_{ABr}^T B_{ABr} + \rho_C I_C B_{Cr}^T B_{Cr} \Big] dx \tag{47}$$

and B_{ij}, $i = A,B,C, j = tx,tz,r$ are translation in x and z directions and rotatory derivative operators for upper and lower faces and core, respectively. $\ddot{q}$ is the acceleration vector.

Equation (39) of the external forces work is discretized as follows

$$\delta W = \delta q^T F_m \tag{48}$$

where F_m is the mechanical external distributed forces/moments vector

$$F_m = \int_0^L \Big[n_A B_{Atx}^T + n_B B_{Btx}^T + n_C B_{Ctx}^T + (q_A + q_B + q_C) B_{tz}^T - (m_A + m_B) B_{ABr}^T + m_C B_{Cr}^T \Big] dx \tag{49}$$

The equivalent electric work δH_{me} can be discretized as follows:

$$\delta H_{me} = \delta q^T F_e \tag{50}$$

where F_e is the induced electric forces/moments vector

$$F_e = \int_0^L \left[e_{31}^{A*} A_A \frac{\tilde{\varphi}_A}{h_A} B_{Am}^T + e_{31}^{B*} A_B \frac{\tilde{\varphi}_B}{h_B} B_{Bm}^T + e_{15}^{C} A_C \frac{\tilde{\varphi}_C}{h_C} B_{Cs}^T \right] dx \tag{51}$$

Using Equations (43), (46), (48) and (50), Equation (42), expressed in matrix form reduces to solve the following linear problem:

$$M\ddot{q} + Kq = F_m - F_e \tag{52}$$

Stiffness and mass [Equations (44) and (47)] matrices, and mechanical and induced electric [Equations (49) and (51)] force/moment vectors were first evaluated exactly (i.e., analytically). However, a shear locking was observed when the core tends to be thin. To solve this problem, the last term of Equation (44), corresponding to the shear stiffness was integrated numerically with only two-point quadrature rule instead of three-point exact numerical integration. All remaining integrals were kept exactly integrated. Good results have then been obtained even for thin cores as it will be shown in the subsequent section.

VALIDATION OF THE FINITE ELEMENT MODEL

A sandwich beam finite element capable of treating both *shear* and *extension actuation mechanisms*, was implemented. In order to validate it, comparisons between present element results and analytical and numerical results found in the literature, were made. Analytical and numerical results for static actuation of continuous [19] and segmented [15] configurations of cantilever beams were presented by Sun and Zhang [15,19]. Modal analysis of segmented configuration of cantilever beams were presented by Lin et al. [12]. For all cases, in the *extension actuation mechanism*, top and bottom layers are supposed to be PZT5H piezoelectric material and the central core to be aluminium. Whereas, for the *shear actuation mechanism*, top and bottom layers are assumed to

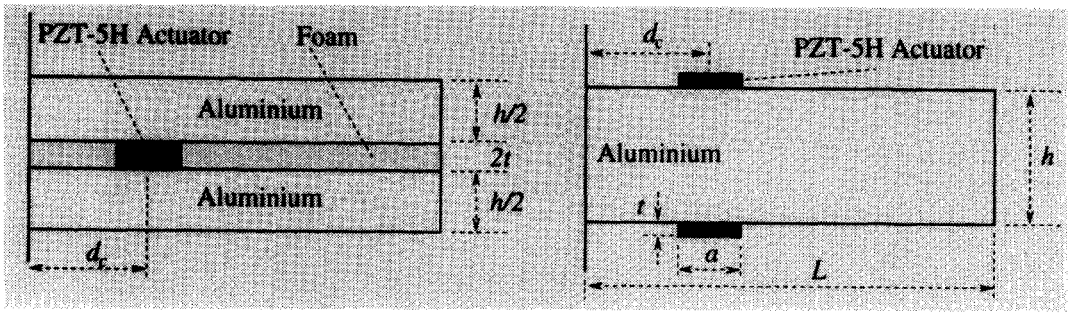

a) Shear Actuation Mechanism b) Extension Actuation Mechanism

Figure 3. *Cantilever sandwich beam, shear and extension actuation mechanisms.*

be aluminium and the central core to be composed of a small patch of PZT5H piezoelectric material and, covering the rest of the core, a rigid foam material. Materials properties are given in the Appendix.

Static Analysis

The geometric configurations of both actuation mechanisms are presented in Figure 3 with $L = 100$ mm, $h = 16$ mm and $t = 1$ mm. Beams are clamped at $x = 0$ and free at $x = L$. In order to bend the beam, voltages are applied at top and bottom surfaces of piezoelectric layers, inducing bending electric forces. For the *shear actuation mechanism*, voltage applied to the piezoelectric core has a value of $V = 20$ V, and for the *extension actuation mechanism*, voltages applied to surface actuators are $V = \pm 10$ V.

As a first analysis, the deflection of both beams for the continuous case, that is, with actuators having the beam's length, was evaluated and compared to analytical results of Reference [19]. In this case, for the *shear actuation mechanism*, there is no rigid foam since the piezoelectric actuator occupies all the core layer.

Finite element results for the transverse displacement of the shear actuated beam match very well with the theoretical solution [19] [Figure 4(a)]. A representation of the magnified deformed configuration of the beam is drawn in Figure 4(b) to show how the actuation of the piezoelectric core causes the bending of the sandwich beam. Finite element results for the transverse displacement of the extension actuated beam match very well with the theoretical solution [19] [Figure 5(a)]. A representation of the magnified deformed configuration of the beam was drawn in Figure 5(b) to show how the actuation of the piezoelectric surface layers causes the bending of the sandwich beam.

As a second analysis, actuator's position is set to vary. In each case, shear actuated beam's tip displacement induced by applied electric forces is evaluated. Actuator's length is fixed at $a = 10$ mm and actuator's position is set to vary in the range [10,90] mm. It can be seen in Figure 6, that present finite element results show very good agreement with finite element results presented in Reference [15], using a commercial finite element code.

Modal Analysis

Natural modes and frequencies were evaluated for both *shear* and *extension actuation mechanisms*. Since it was not found in the literature evaluation of eigenfrequencies and modes for the *shear actuation mechanism*, only the *extension actuation mechanism* numerical eigenfrequencies were

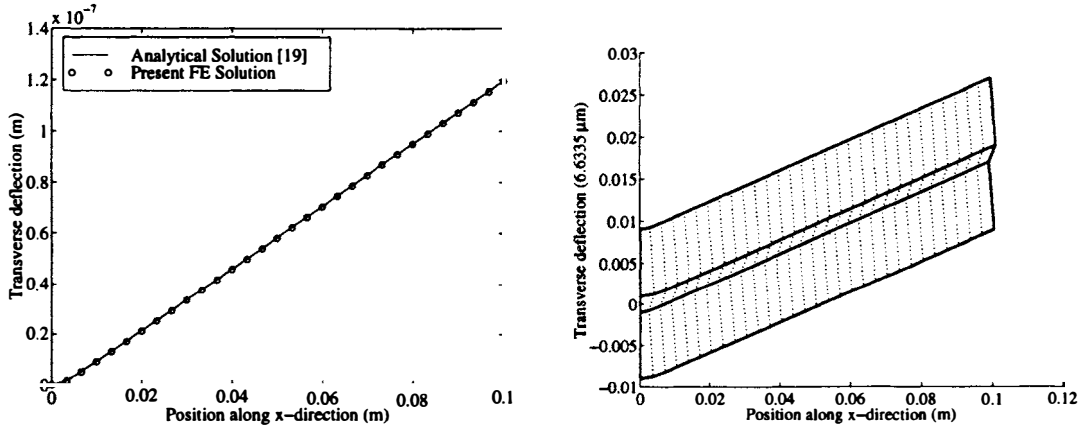

(a) (b)

Figure 4. *(a) Transverse displacement of the beam and (b) deformed configuration of the beam.*

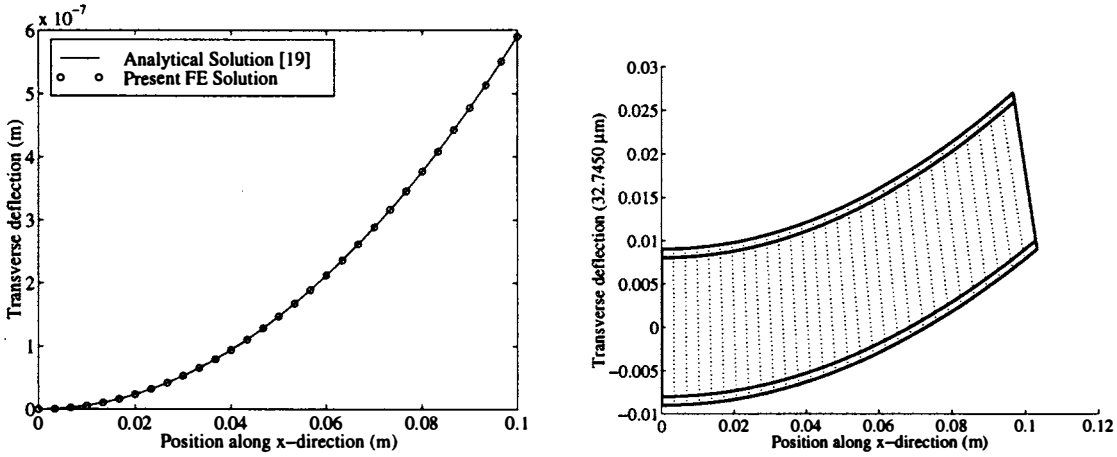

Figure 5. *(a) Transverse displacement of the beam and (b) deformed configuration of the beam.*

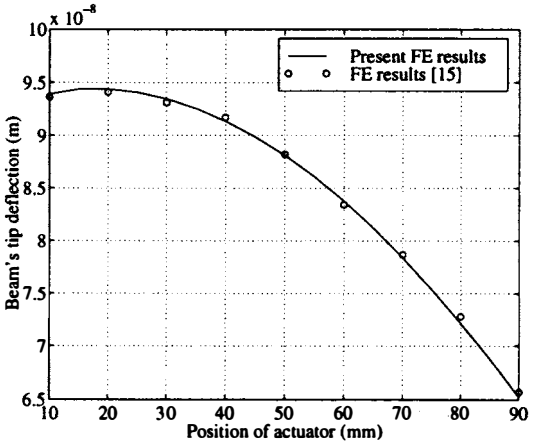

Figure 6. *Beam's tip transverse displacement for actuator's several positions.*

Table 1. First five natural bending frequencies (Hz) for shear and extension actuated cantilever beam.

		Freq. 1	Freq. 2	Freq. 3	Freq. 4	Freq. 5
Shear actuation	Present FE results	989	3916	8374	17416	26025
Extension actuation	Present FE results	1084	4430	12422	23499	38014
	Analytical results [12]	1030	4230	12000	23500	38500
	Error (%)	5.24	4.73	3.52	−0.00	−1.26

compared to analytical [12] ones. Natural frequencies were also given in Table 1 for the *shear actuation mechanism*. Material data are the same as presented in Reference [12] and geometric parameters are $L = 50$ mm, $h = 2$ mm, $t = 0.5$ mm, $d_c = 11$ mm and $a = 20$ mm. The equivalent shear actuation beam is represented by Figure 3(a). A graphical representation of the first three bending modes is shown in Figure 7. It can be seen that in all three bending modes, actuator's deformation is lower for the *shear actuation mechanism*. The finite element results for the natural bending frequencies showed good agreement with analytical ones (Table 1).

CONCLUSIONS

A theoretical formulation and finite element implementation of a new adaptive unsymmetric sandwich beam model were presented and validated, for both *extension* and *shear actuation mechanisms*. Mechanically, the model is based on Bernoulli-Euler assumptions in the faces and Timoshenko hypotheses in the core. Rotary inertia effects were considered for all layers. Electrically, the electric potential was found to be quadratic for *extension actuation mechanism* (piezoelectric faces) and linear for *shear actuation mechanism* (piezoelectric core). Besides, the sandwich beam was supposed to be short circuited, i.e., electric potentials were imposed on upper and lower faces of piezoelectric layers and natural boundary conditions (free-charge) were assumed on the remaining lateral boundaries.

It was found that piezoelectric effects modify the bending stiffness of the sandwich beam due to the induced potentials and induce a sort of "initial" electric stress-state which can be seen also as a generalized electric forces work. For the actuation problem, all energy and work variations are written in terms of three main variables; namely, mean and relative axial displacements of the upper and lower core's skins and the transverse deflection of the beam. Augmented by the bending Bernoulli-Euler rotation, these are the only finite element dof, i.e., there was no use of additional electric dof.

The present adaptive sandwich finite element was used to study static deflection of a cantilever sandwich beam under extension and shear actuation conditions. The results show good comparisons to the analytic results found in the literature. Deformations of the sandwich beam were also shown to illustrate both *extension* and *shear actuation mechanisms*. It was also found that the induced potential in the faces increases the rigidity of the global structure. Dynamic analysis of both actuation mechanisms was also presented, through evaluation of natural bending frequencies and modes. Numerical results showed good agreement with analytical ones. Vibration modes are equivalent in both mechanisms; nevertheless shear actuators are less deformed than extension ones.

Careful comparisons of two cantilever beams with equivalent geometrical and material properties and under equiva-

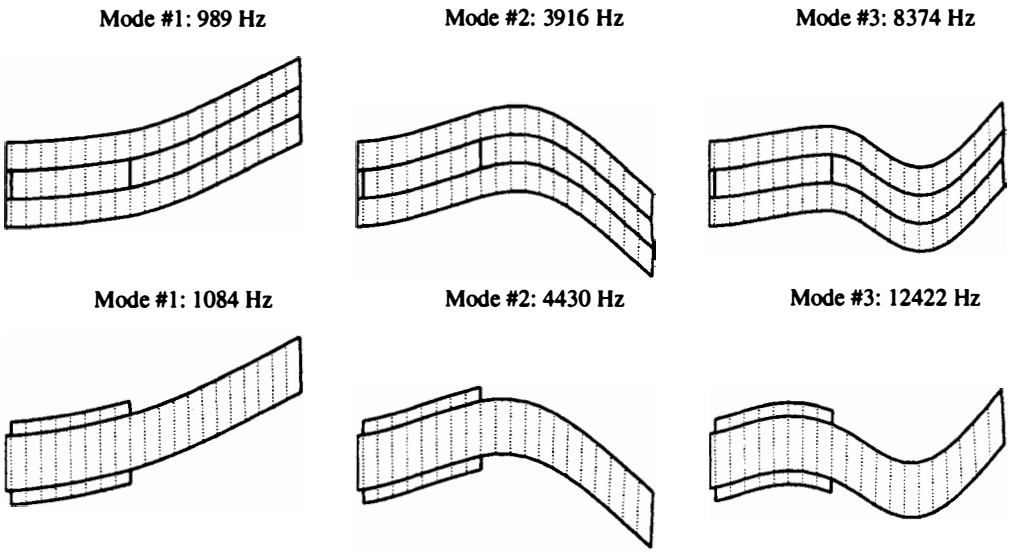

Figure 7. Natural bending modes and frequencies for shear and extension actuation mechanisms.

lent electrical boundary conditions, indicate that the shear-actuated beam is less deformed (smaller tip's maximum transverse displacement). Hence, the bending stress is also smaller which is an advantage for brittle piezoceramics. The shear actuator mechanism induces also extra shear strains which are another benefit for energy dissipation purposes.

The present work is being extended to implement the sensoring capacity of the adaptive sandwich beam in order to study active control applications. A second adaptive sandwich beam model, taking into account the extra-shear due to the sliding of the faces against the core, has also been developed in order to augment energy-dissipation capacity of the beam [5].

APPENDIX

Constitutive Equations

For transversely polarized piezoelectric material, converse and direct effects constitutive equations have the following form

$$\left[\begin{array}{c|c} \sigma_1 \\ \sigma_2 \\ \sigma_3 \\ \sigma_4 \\ \sigma_5 \\ \sigma_6 \\ \hline D_1 \\ D_2 \\ D_3 \end{array}\right] = \left[\begin{array}{ccccc|cccc} c_{11} & c_{12} & c_{13} & 0 & 0 & 0 & 0 & 0 & -e_{31} \\ c_{12} & c_{22} & c_{23} & 0 & 0 & 0 & 0 & 0 & -e_{32} \\ c_{13} & c_{23} & c_{33} & 0 & 0 & 0 & 0 & 0 & -e_{33} \\ 0 & 0 & 0 & c_{44} & 0 & 0 & 0 & -e_{24} & 0 \\ 0 & 0 & 0 & 0 & c_{55} & 0 & -e_{15} & 0 & 0 \\ 0 & 0 & 0 & 0 & 0 & c_{66} & 0 & 0 & 0 \\ \hline 0 & 0 & 0 & 0 & e_{15} & 0 & \epsilon_1 & 0 & 0 \\ 0 & 0 & 0 & e_{24} & 0 & 0 & 0 & \epsilon_2 & 0 \\ e_{31} & e_{32} & e_{33} & 0 & 0 & 0 & 0 & 0 & \epsilon_3 \end{array}\right] \left[\begin{array}{c} \varepsilon_1 \\ \varepsilon_2 \\ \varepsilon_3 \\ \varepsilon_4 \\ \varepsilon_5 \\ \varepsilon_6 \\ \hline E_1 \\ E_2 \\ E_3 \end{array}\right] \tag{A1}$$

where σ, ε, D and E are stress, strain symmetric tensors and electric displacement and field vectors. c_{ij}, e_{kj} $(i,j = 1,\ldots,6)$ and ϵ_k $(k = 1,2,3)$ denote, respectively, elastic, piezoelectric and dielectric material constants.

If a piezoelectric material is poled in its axial direction (1 or x), its constitutive equations can be obtained from Equation (A1), through a 90° rotation around the second direction (2 or y) followed by a 180° rotation around the third direction (3 or z). Applying successively these rotations to Equation (A1), we get [9]

$$\left[\begin{array}{c|c} \sigma_1 \\ \sigma_2 \\ \sigma_3 \\ \sigma_4 \\ \sigma_5 \\ \sigma_6 \\ \hline D_1 \\ D_2 \\ D_3 \end{array}\right] = \left[\begin{array}{ccccc|cccc} c_{33} & c_{23} & c_{13} & 0 & 0 & 0 & -e_{33} & 0 & 0 \\ c_{23} & c_{22} & c_{12} & 0 & 0 & 0 & -e_{32} & 0 & 0 \\ c_{13} & c_{12} & c_{11} & 0 & 0 & 0 & -e_{31} & 0 & 0 \\ 0 & 0 & 0 & c_{66} & 0 & 0 & 0 & 0 & 0 \\ 0 & 0 & 0 & 0 & c_{55} & 0 & 0 & 0 & -e_{15} \\ 0 & 0 & 0 & 0 & 0 & c_{44} & 0 & -e_{24} & 0 \\ \hline e_{33} & e_{32} & e_{31} & 0 & 0 & 0 & \epsilon_3 & 0 & 0 \\ 0 & 0 & 0 & 0 & 0 & e_{24} & 0 & \epsilon_2 & 0 \\ 0 & 0 & 0 & 0 & e_{15} & 0 & 0 & 0 & \epsilon_1 \end{array}\right] \left[\begin{array}{c} \varepsilon_1 \\ \varepsilon_2 \\ \varepsilon_3 \\ \varepsilon_4 \\ \varepsilon_5 \\ \varepsilon_6 \\ \hline E_1 \\ E_2 \\ E_3 \end{array}\right] \tag{A2}$$

Material Properties

ALUMINIUM

Density: $\rho = 2690$ kg m^{-3}; Young's modulus: $E = 70.3$ GPa; Poisson's coefficient: $\nu = 0.345$.

RIGID FOAM

Density: $\rho = 32$ kg m^{-3}; Young's modulus: $E = 35.3$ MPa; Shear modulus: $G = 12.76$ MPa.

PZT5H

$$\mathbf{c} = \begin{bmatrix} 12.6 & 7.95 & 8.41 & 0 & 0 & 0 \\ & 12.6 & 8.41 & 0 & 0 & 0 \\ & & 12.6 & 0 & 0 & 0 \\ & & & 2.33 & 0 & 0 \\ & sym & & & 2.3 & 0 \\ & & & & & 2.3 \end{bmatrix} \times 10^{10} \text{ N m}^{-2}$$

$$\mathbf{e} = \begin{bmatrix} 0 & 0 & 0 & 0 & 0 & 17 \\ 0 & 0 & 0 & 0 & 17 & 0 \\ -6.5 & -6.5 & 23.3 & 0 & 0 & 0 \end{bmatrix} \text{C m}^{-2}$$

$$\epsilon = \begin{bmatrix} 1.503 & 0 & 0 \\ 0 & 1.503 & 0 \\ 0 & 0 & 1.3 \end{bmatrix} \times 10^{-8} \text{ F m}^{-1}$$

PIEZOELECTRIC MATERIAL OF THE MODAL ANALYSIS PROBLEM

Density: $\rho = 7730$ kg m^{-3}

$$\mathbf{c} = \begin{bmatrix} 12.8 & 6.6 & 6.6 & 0 & 0 & 0 \\ & 12.8 & 6.6 & 0 & 0 & 0 \\ & & 11.0 & 0 & 0 & 0 \\ & & & 2.1 & 0 & 0 \\ & sym & & & 2.1 & 0 \\ & & & & & 2.1 \end{bmatrix} \times 10^{10} \text{N m}^{-2}$$

REFERENCES

1. Baz, A. 1997. "Boundary Control of Beams Using Active Constrained Layer Damping," *J. Vib. Acoust.*, 119:166–172.
2. Benjeddou, A., M. A. Trindade and R. Ohayon. 1997. "A Finite Element Model for Extension and Shear Piezoelectrically Actuated Adaptive Structures," *Japan-France Seminar on Intell. Mater. Struct.*, 277–295.
3. Benjeddou, A., M. A. Trindade and R. Ohayon. 1997. "A Finite Element Model for Shear Actuated Adaptive Structures," *8th Int. Conf. Adaptive Struct. Tech.*, Wakayama, Japan, Technomic Publishing Co, Inc. (in press).
4. Benjeddou, A., M. A. Trindade and R. Ohayon. 1998. "Comparison of Extension and Shear Actuation Mechanisms for Smart Structure Beams," *4th European Conf. on Smart Struct. & Mater.*, July 6–8, Harrogate, UK (to be presented).
5. Benjeddou, A., M. A. Trindade and R. Ohayon. 1998. "Finite Element Modeling of Shear Actuated Structures," *39th AIAA/ASME/ASCE/AHS/ASC Structures, Structural Dynamics, and Materials Conference*, April 20–23, Long Beach, CA, AIAA paper #98-1922.
6. Crawley, E. F. and J. de Luis. 1987. "Use of Piezoelectric Actuators as Elements of Intelligent Structures," *AIAA J.*, 25(10):1373–1385.
7. Crawley, E. F. and E. H. Anderson. 1990. Detailed Models of Piezoceramic Actuation Beams," *J. Intell. Mater. Syst. Struct.*, 1:4–25.
8. Dosch, J. J., D. J. Inman and E. Garcia. "A Self-Sensing Piezoelectric Actuator for Collocated Control," *J. Intell. Mater. Syst. Struct.*, 3:166–185.
9. Hagood, N., R. Kindel, K. Ghandi and P. Gaudenzi. 1993. "Improving Transverse Actuation of Piezoceramics Using Interdigitated Surface Electrodes," *North American Conf. on Smart Struct. & Mater.*, N. W. Hagood, G. J. Knowles, eds., SPIE 1917:341-352.
10. Herman Shen, M.-H. 1994. "Analysis of Beams Containing Piezoelectric Sensors and Actuators," *Smart Mater. Struct.*, 3:439–447.
11. Herman Shen, M.-H. 1995. "A New Modeling Technique for the Piezoelectrically Actuated Beams," *Comp. & Struct.*, 57(3):361-366.
12. Lin, M. W., A. O. Abatan and C. A. Rogers. 1994. "Application of Commercial Finite Element Codes for the Analysis of Induced Strain-Actuated Structures," *2nd Int. Conf. Intell. Mater.*, Technomic Publishing Co., Inc., 846–855.
13. Rahmoune, M., D. Osmont, A. Benjeddou and R. Ohayon. 1996. "Finite Element Modeling of a Smart Structure Plate System," *7th Int. Conf. Adaptive Struct. Tech.*, Technomic Publishing Co., Inc., 463–473.
14. Soong, T. T. and R. D. Hanson. 1993. "Recent Development in Active and Hybrid Control Research in the U.S.," *Int. Workshop on Struct. Control*, 483-490.
15. Sun, C. T. and X. D. Zhang. 1995. "Use of Thickness-Shear Mode in Adaptive Sandwich Structures," *Smart Mater. Struct.*, 4:202–206.
16. Warkentin, D. J. and J. Tani. 1997. "Rainbow Actuators for Acoustic Control: The Active Wall Concept," *8th Int. Conf. Adaptive Struct. Tech.*, Wakayama, Japan, Technomic Publishing Co., Inc. (to appear).
17. Yang, S. M. and Y. J. Lee. 1994. "Interaction of Structure Vibration and Piezoelectric Actuation," *Smart Mater. Struct.*, 3:494–500.
18. Yang, S. M. and Y. J. Lee. 1996. "Structural Vibration Suppression by Concurrent Piezoelectric Sensors and Actuators," *Smart Mater. Struct.*, 5:806–813.
19. Zhang, X. D. and C. T. Sun. 1996. "Formulation of an Adaptive Sandwich Beam," *Smart Mater. Struct.*, 5:814–823.